Contents lists available at ScienceDirect

Comptes Rendus Biologies

www.sciencedirect.com

Biological modelling/Biomodélisation

Modeling of the effects of IL-17 and TNF-α on endothelial cells and thrombus growth

Modélisation des effets des cytokines IL-17 and TNF-α sur les cellules endothéliales et la croissance du thrombus

Anass Bouchnita [a,b,*], Pierre Miossec [c], Alen Tosenberger [d], Vitaly Volpert [e,f,g]

[a] Laboratoire de biométrie et biologie évolutive (LBBE), UMR 5558 CNRS, Université Lyon-1, 69376 Lyon, France
[b] Mohammadia School of Engineering (EMI), Université Mohammed-V, 10080 Rabat, Morocco
[c] Department of Clinical Immunology and Rheumatology, Immunogenomics and Inflammation, Research Unit EA 4130, Hôpital Édouard-Herriot, Université de Lyon, 69437 Lyon, France
[d] Unité de chronobiologie théorique, Faculté des sciences, Université ibre de Bruxelles (ULB), campus Plaine, CP 231, 1050 Bruxelles, Belgium
[e] Institut Camille-Jordan (ICJ), UMR 5208 CNRS, Université Lyon-1, 69622 Villeurbanne, France
[f] Intitut national de recherche en informatique et automatique (INRIA), Team Dracula, INRIA Lyon La Doua, 69603 Villeurbanne, France
[g] RUDN University, ul. Miklukho-Maklaya 6, 117198 Moscow, Russia

A R T I C L E   I N F O

A B S T R A C T

Rheumatoid and psoriatic arthritis are chronic inflammatory diseases, with massive increase of cardiovascular events (CVE), and contribution of the cytokines TNF-α and IL-17. Chronic inflammation inside the joint membrane or synovium results from the activation of fibroblasts/synoviocytes, and leads to the release of cytokines from monocytes (Tumor Necrosis Factor or TNF) and from T lymphocytes (Interleukin-17 or IL-17). At the systemic level, the very same cytokines affect endothelial cells and vessel wall. We have previously shown [1,2] that IL-17 and TNF-α, specifically when combined, increase procoagulation, decrease anticoagulation and increase platelet aggregation, leading to thrombosis. These results are the basis for the models of interactions between IL-17 and TNF, and genes expressed by activated endothelial cells. This work is devoted to mathematical modeling and numerical simulations of blood coagulation and clot growth under the influence of IL-17 and TNF-α. We show that they can provoke thrombosis, leading to the complete or partial occlusion of blood vessels. The regimes of blood coagulation and conditions of occlusion are investigated in numerical simulations and in approximate analytical models. The results of mathematical modeling allow us to predict thrombosis development for an individual patient.

R É S U M É

Les polyarthrites rhumatoïdes et psoriasques sont des maladies inflammatoires chroniques, caractérisées par une augmentation massive du risque d'événements cardiovasculaires (ECV) et par une contribution des cytokines TNF-α et IL-17. L'inflammation chronique à l'intérieur de la synoviale articulaire, ou membrane, conduit à l'activation des fibroblastes/synoviocytes et mène à la libération de cytokines par des monocytes (facteur de nécrose tumorale ou TNF) et des lymphocytes T (interleukine-17 ou

* Corresponding author.
E-mail address: anass.bouchnita@univ-lyon1.fr (A. Bouchnita).

IL-17). Au niveau systémique, les mêmes cytokines affectent les cellules endothéliales et la paroi du vaisseau. Nous avons précédemment montré [1,2] que l'IL-17 et le TNF-α, en particulier lorsqu'ils sont combinés, favorisent l'activité procoagulante, diminuent l'anticoagulation et augmentent l'agrégation plaquettaire, ce qui conduit au développement d'une thrombose. Ce constat est basé sur des modèles d'interactions entre IL-17, TNF-α et des gènes exprimés par des cellules endothéliales activées. Ce travail est consacré à la modélisation mathématique et à la simulation numérique de la coagulation sanguine et de la croissance du caillot sanguin sous l'influence de l'IL-17 et TNF-α. Nous montrons qu'ils peuvent provoquer une thrombose conduisant à l'occlusion complète ou partielle des vaisseaux sanguins. Les régimes de coagulation du sang et les conditions d'occlusion sont examinés par des simulations numériques et à travers des modèles analytiques approximatifs. Les résultats de la modélisation mathématique permettent de prédire le développement de la thrombose chez un patient individuel.

1. Introduction

1.1. Inflammation and cardiovascular risk (CV risk) are increased in RA and PsA

The impact of cardiovascular (CV) diseases on the society is enormous, and any method able to identify early individuals at risk will have a significant effect on morbidity and mortality. Classical CV risk factors related to obesity, hypertension, smoking, etc., have been identified for a long time. More recently, chronic inflammation has become an important link between these risk CV factors and the actual CV events. For many years, rheumatoid and psoriatic arthritis (RA, PsA) as well as similar diseases have been linked to local damage and to function loss. The goal of arthritis care was the control of local inflammation in order to prevent loss of joint function. It is unclear why it took so long to look at patient survival. When compared to control populations, it was obvious that life expectancy was severely affected [3]. Quickly joint destruction and mortality were linked to the level and duration of inflammation [4].

The most common cause of death in RA, PsA, and similar diseases is vascular disease, contributing 60% of the mortality risk in RA patients, comparable to diabetes mellitus as an independent risk factor for CV disease. RA patients have a four-fold increase in CV mortality. Figures are even higher when considering only RA patients who are rheumatoid factor positive or with high CRP levels [4]. In addition, this risk begins very early in the RA disease process [5]. In total, the prevalence of CV disease in RA has been found to be 16.2%. However, the largest difference in CV between RA patients and controls is seen in those without traditional risk factors – patients who are young, female, and have a low body mass index [6]. With specific regards to cardiac disease, RA patients have a twofold higher risk of myocardial infarction (MI) as compared to controls [5]. The odds ratio of having a MI with RA, as opposed to that with osteoarthritis (OA), a less inflammatory joint disease, is 2.14, and the odds ratio of having a MI at some point in life, again as compared to patients with OA, is 1.28 for RA patients (30). RA patients also carry a twofold higher risk of chronic heart failure (CHF) [5]. The odds ratio of having CHF with RA, as opposed to with OA, is 1.43 [7].

1.2. Effects of the cytokines TNF and IL-17 on vessels

Chronic inflammatory diseases are associated with overproduction of cytokines. These factors have a direct effect on the local manifestations that lead to joint destruction. As a consequence, targeting of TNF and more recently of IL-17 has provided an important improvement in care. In addition to the local effects, the same cytokines have also systemic effects. Circulating cytokines can then act on endothelial cells. Our previous research has studied the effects of TNF and IL-17, used alone and combined on human endothelial cells (EC). We recently showed that IL-17, especially when combined with TNF, has procoagulant, pro-aggregation, and pro-thrombotic effects [1,2]. All these effects are inhibited by the addition of statins [1,2]. IL-17 may play a significant role in the development of endothelial dysfunction and cardiovascular disease [8]. In apoE-deficient mice that have major vessel disease, IL-17A-blocking antibody reduced atherosclerotic lesion development, plaque vulnerability, cellular infiltration, and tissue activation [9]. IL-17 deficient mice, when on high fat diet, displayed significantly diminished aortic lesion size and macrophage accumulation [10].

Expanding these results to the human situation, a high peak of IL-17 plasma level was found in patients with unstable angina, if followed by myocardial infarction [11]. Thrombosis is the result of platelet aggregation and pro-coagulation activation in EC. To study the role of IL-17 in platelet aggregation, a functional assay with platelet-rich plasma (PRP) was performed. Supernatants of EC treated with IL-17 and TNF were added to PRP and ADP, acting as an agonist of platelet aggregation. Aggregation was monitored by changes in light transmittance in a lumiaggregometer. IL-17 alone enhanced the level of platelet aggregation from 20% to 45–50% ($P = 0.001$). A similar effect was seen with TNF combined with IL-17. Regarding the effects on coagulation, IL-17 and TNF induced synergistically a massive expression of the tissue factor (F3, 15-fold), a key player to initiate the coagulation cascade. Furthermore, IL-17 and TNF induced plasminogen

activator mRNA expression by 6-fold with an additive effect. Conversely, IL-17 in combination with TNF inhibited by 10-fold the expression of thrombomodulin, an inhibitor of coagulation, thus increasing the EC pro-thrombotic phenotype. Microarrays identified CD39, an inhibitor of platelet aggregation, among the genes inhibited by IL-17. The preserved function of CD39/ATPDase is crucial in the inhibition of platelet activation by keeping adenosine nucleotide levels low to inhibit platelet aggregation. After 12 h of incubation with IL-17, TNF and their combination, CD39mRNA expression was divided by 3.7. Thus, IL-17A was able to induce an imbalance between a pro-thrombotic and anticoagulant phenotype. These results were the basis for the development of the models of interactions between IL-17 and TNF, and the genes expressed by activated EC.

1.3. Coagulation cascade

Endothelial cells of the vessel wall produce tissue factor (T_f, T_f), tissue factor pathway inhibitor (TFPI), thrombo-modulin (T_m, T_m) and CD39. T_f acts as the initiator of the blood clotting process in blood plasma by activating factors IX and X (B). The resulting enzymes activate prothrombin (P) which is produced in liver and circulates in the bloodstream, and creates thrombin (T). A low amount of thrombin is able to rapidly generate more thrombin in a self-accelerated reaction. Thrombin then acts as an enzyme in activation of fibrinogen (F_g) to fibrin (F). Through a polymerization process, fibrin monomers create a net of fibrin polymers (F_p) that solidifies blood plasma. This mechanism ensures a quite rapid closure of possible vessel wall injuries and reduces a potential blood loss. We have shown the part of the coagulation cascade considered in this work in Fig. 1. Blood coagulation needs to be triggered only in situations when it is necessary, while otherwise it needs to be prevented. Blood haemostasis

hangs on a delicate balance of the involved blood factors, and as such it needs to be quite robust.

There are multiple fail-safe mechanisms that prevent spontaneous blood coagulation and limit the clot growth in the case of an injury (preventing vessel occlusion). The first one is the production of TFPI by EC, which acts as an inhibitor of T_f and prevents the initiation of the coagulation process. CD39 prevents adhesion of platelets to the vessel wall. Protein C is activated in the presence of thrombin and inhibits slowly thrombin generation. However, in the presence of thrombomodulin, which is also produced by EC, the activation of protein C is increased by a factor of one thousand, hence increasing the inhibition of thrombin production. Another mechanism is the direct inhibition of thrombin by antithrombin (AT, A).

In the case of the vessel wall inflammation due to presence of IL-17 and TNF-α in the blood stream, the EC are affected and their production of blood factors is altered. The production of procoagulation factors is increased, while the production of anticoagulation factors is severely decreased. Additionally, the production of TFPI and CD39 is reduced, allowing the platelets to more easily adhere to the vessel wall and disabling the haemostatic system in preventing spontaneous coagulation.

1.4. Modeling, using the in vitro results

In this work, we develop a model and carry out numerical simulations of clot growth taking into account the influence of IL-17 and TNF. We show that they promote blood coagulation and clot growth and they can lead to partial or complete vessel occlusion. We develop a simplified analytical model that allows us to obtain explicit conditions of thrombosis. We have previously used the same approach to determine the conditions on prothrombin and antithrombin that potentially result in exaggerated or insufficient thrombus development
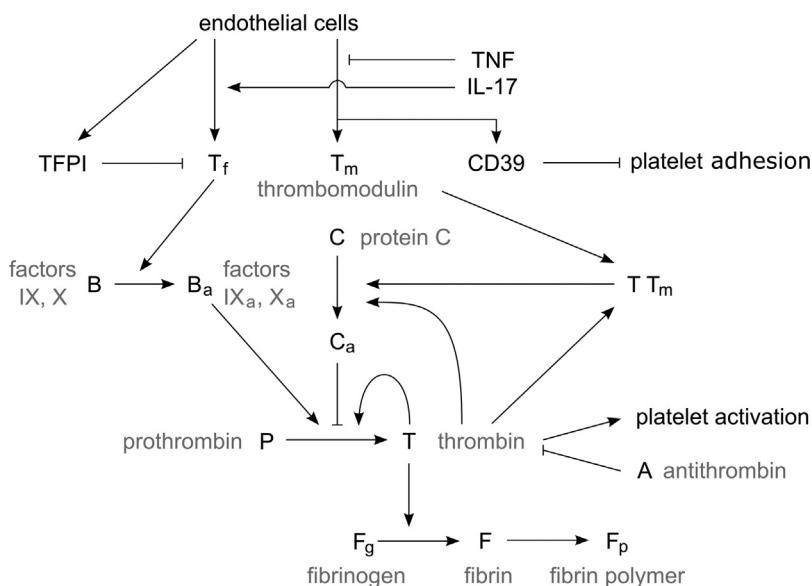

Fig. 1. Simplified representation of blood coagulation (see the explanation in the text).

[12]. Various approaches are employed to study clot growth. Equations of chemical kinetics are used to describe reactions between the coagulation factors [13,14], platelet activation, and formation of platelets plug [15]. Reaction–diffusion equations for the concentrations of blood factors take into account their spatial distribution [16,17]. These distributions are influenced by hemodynamics. The blood flow can be modeled with partial differential equations or with particle methods. Navier–Stokes equations are used if blood is considered as a Newtonian fluid [18,19], and various viscoelastic models if non-Newtonian properties of blood are taken into account [18,20]. Clot growth can be modeled as a free boundary problem where the interface separates the blood flow from the clot region [21].

Another approach considers the blood flow and the clot as a continuous medium where clot is described as a high viscosity or a non-Newtonian fluid [18,22]. Clot can also be described as a porous medium with an additional term in the Navier–Stokes equations [23] describing fluid velocity deceleration inside the clot. In order to model platelets, both particle and continuous methods were used. Among the particle methods, the Immersed Boundary Method was used in [24], Cellular Potts Model [25], Dissipative Particle Dynamics in [20,26–29]. Advection–diffusion–reaction were also used to model platelet concentration (in their active and non-active forms) [15]. In hybrid models, particle methods are used to describe the blood flow and the blood cells and PDEs to describe concentrations of blood factors [27,28]. It is also possible to model the blood flow with the Navier–Stokes equations and the coagulation process with Cellular Automata [25].

In this work, we begin with the analysis of blood coagulation in quiescent platelet free plasma in order to determine the influence of IL-17 and TNF-α and identify the values of parameters (Section 2.1). We continue with numerical simulations of blood coagulation in flow using two different approaches. In the first one, the blood flow is described with the Navier–Stokes equations, while the concentrations of blood factors and of platelets with reaction–diffusion equations (Section 2.2). In the second

approach, the blood flow and the platelets are modeled with a particle method, while the distribution of blood factors, as before, with reaction–diffusion equations (Section 3). The first method is more appropriate to study venous thrombosis with relatively low blood flow velocity. The second method is better for arteries and larger flow velocities where platelet aggregation is more important. We describe here platelets interaction (forces, attachment, detachment) in more detail. Numerical simulations are completed by an approximate analytical approach that allows us to identify different regimes of clot growth and conditions of vessel occlusion (Section 4).

2. Modeling blood coagulation and thrombosis

In the mathematical model of blood coagulation, we consider a rectangular 2D domain representing a section of a blood vessel. The source of blood factors can be either at the inflow boundary, if they are produced elsewhere and circulate in the blood stream, or at the vessel wall, if they are produced there under normal and pathologic conditions (vessel wall injury, vessel wall inflammation).

2.1. Clot growth in quiescent plasma

The evolution of thrombin concentration in time (without space distribution) is one of the main characteristics of blood coagulation in plasma. In Fig. 2a, we compare the thrombin generation profile of a healthy patient with those with perturbed tissue factor (T_f) and thrombomodulin (T_m) concentrations due to IL-17 and TNF-α [30]. The results show that in the absence of spatial dynamics, hypercoagulability is more increased by IL-17 than by TNF-α. The highest thrombosis risk was observed when the effect of the two proteins is combined. Through fitting the thrombin generation curves, we estimated that RA increases the concentration of T_f by a factor of two, while it decreases the concentration of T_m by 20%.

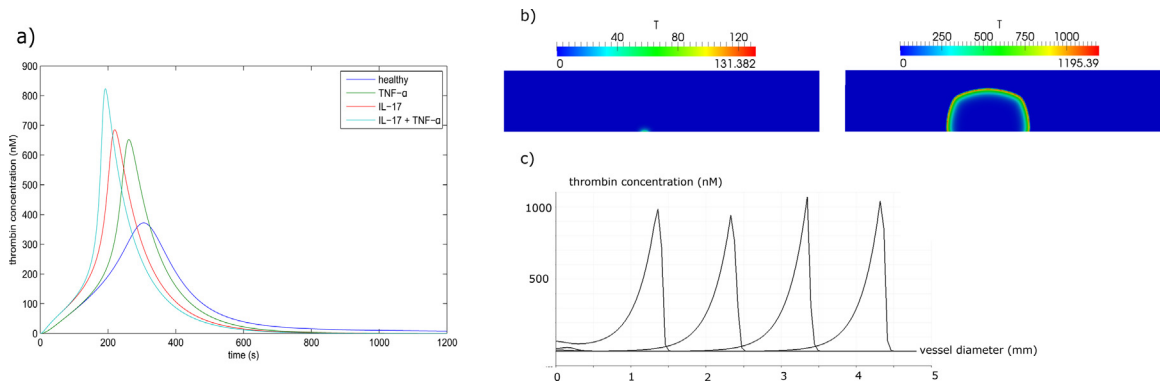Next, we consider clot growth in quiescent plasma in a rectangular domain representing a part of blood vessel.

Fig. 2. (a) Thrombin generation curves in the normal case and in the excess of IL-17, TNF-α and their combination. (b) Thrombin distribution during clot formation in a quiescent plasma. In the presence of IL-17, only a small clot forms near the wall, while if IL-17 and TNF-α are both present, the clot grows up to the opposite wall of the vessel, resulting in complete occlusion. (c) Thrombin distribution along the middle line of the clot (perpendicular to the vessel wall) in consecutive moments of time.

There is an inflamed part of the vessel wall where T_f is expressed. It is the 0.5-mm-long interval at the center of the lower boundary (Fig. 2b). We compare two cases where the upregulation of T_f due to IL-17 is considered. In the first simulation, we neglect the inhibitory action of TNF-α on thrombomodulin. In spite of the excessive level of T_f due to IL-17, the thrombin wave does not propagate because of the inhibitory action of the activated protein C (APC). It is produced at intact parts of the vessel wall from both sides of the lesion due to the complex of T_m with thrombin. As a result, a small and limited clot forms over the inflamed region (Fig. 2b).

We consider now the case where the action of TNF-α is taken into account. It downregulates the expression of thrombomodulin at the intact neighboring parts of the wall. As a result, the concentration of T_m is reduced, decreasing also the rate of activation of protein C. The generated APC is not sufficient to stop the formation of the clot (Fig. 2b). The distribution of thrombin concentration along the middle line of the clot (perpendicular to the vessel wall) is shown in (Fig. 2c) at successive moments of time. This distribution has a form of localized spike moving from the boundary toward the inside of the vessel. It is a traveling wave solution to the corresponding reaction–diffusion system of equations of blood coagulation. Conversion of fibrinogen into fibrin and clot formation occurs behind the moving zone of thrombin formation.

2.2. The influence of the blood flow

We describe thrombus formation under a pressure-driven blood flow with a low shear rate of $13\,\mathrm{s}^{-1}$. The vessel diameter is set as 1.5 mm. We consider a fixed inflamed region of the blood vessel wall with the length 400 μm. If the inflamed tissue length is relatively small, then the individual actions of IL-17 or TNF-α are not sufficient to trigger the propagation of the clot. Hence, a normal haemostatic response is observed. As a result, a small clot is formed and the flow is not perturbed (not shown).

A joint action of IL-17 and TNF-α initiates clot growth. It can result in the complete occlusion of the vessel. In this case, the velocity profile at the inlet decreases as the clot expands. It vanishes when the thrombus completely occludes the vessel. Fig. 3 shows thrombin distribution (a) and platelets in the clot (b) at three consecutive moments of time. Thrombin distribution resembles that for the case of clot growth in a quiescent plasma, but here the flow breaks the symmetry of thrombin distribution by moving it downstream. The interaction of thrombin and platelets play an important role in clot growth. Thrombin activates platelets and promotes platelet attachment from the flow to the platelets in the clot. Platelet attachment and detachment will be discussed in more detail in the next section. On the other hand, the surface of activated platelets converts prothrombin into thrombin (similar to the vessel wall) reinforcing thrombin production. Thus, there is a positive feedback between thrombin generation and platelet aggregation. Hence, TNF-α reinforces platelet adhesion, especially when combined with IL-17.

The dynamics of clot growth in normal and inflamed cases is shown in Fig. 4. In the normal case (without IL-17, TNF-α), the clot does not grow. Its grows rate is maximal under the joint action of the inflammation factors.
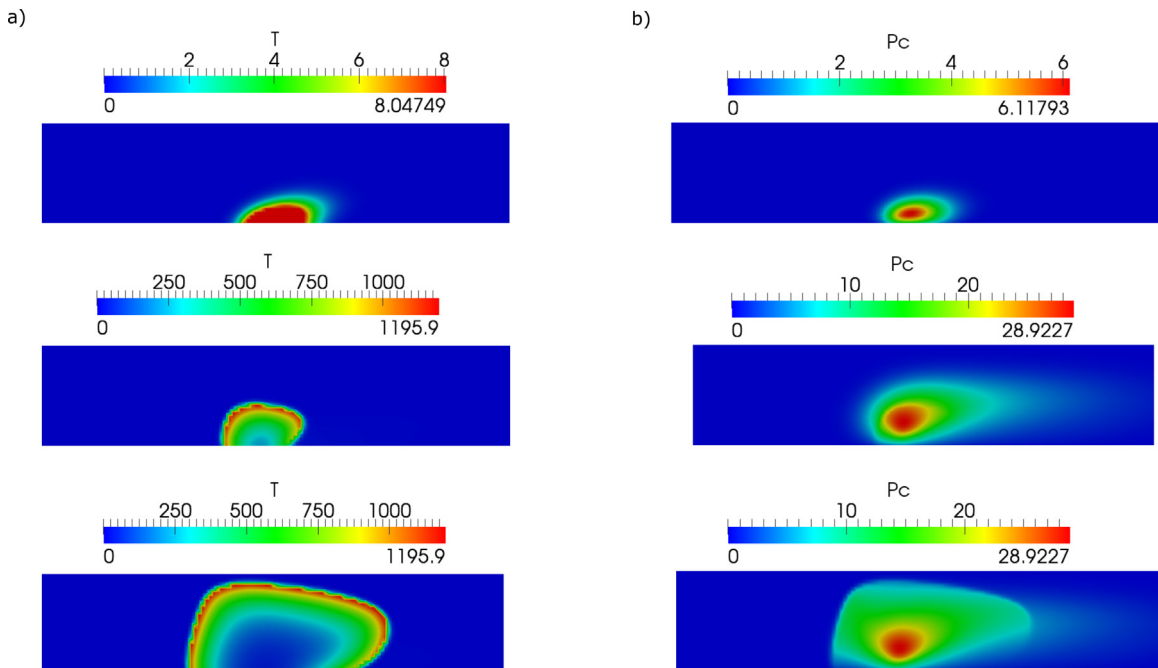

Fig. 3. Clot growth under the joint action of IL-17 and TNF-α. Thrombin distribution (a) and platelet aggregation (b) are shown at consecutive moments of time. The clot fills the whole vessel cross section leading to a complete vessel occlusion.
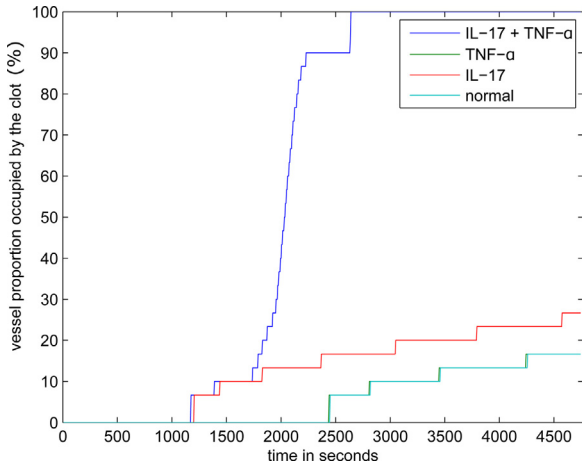
Fig. 4. Dynamics of clot growth in the case of separate or joint action of IL-17 and TNF-α. TNF-α has no effect on thrombus development in quiescent plasma and when the inflamed tissue is sufficiently wide, the corresponding curve coincides with the normal case.

One of the important parameters that determine thrombus formation and growth is the size of the lesion and its evolution in time. There are some experimental data [31] confirmed by modeling [32,33] that show how the risk of vessel occlusion depends on the lesion size. However, it is not known how it grows in time in the case of chronic inflammation. Therefore, we vary this parameter in the model, and we observe its influence on thrombus growth (Fig. 5).

3. Platelet aggregation model

Clot growth consists of two main processes and of their interaction: biochemical reactions in blood plasma resulting in the production of fibrin polymer and platelet aggregation. Platelet aggregation is a complex multi-stage process that consists of different mechanisms. These mechanisms include platelet attachment to the clot and its possible detachment, platelet activation, different adhesion forces acting between platelets due to different receptors involved, platelet interaction with fibrin and some other blood factors. In order to study platelet aggregation in more detail, we use a DPD–PDE model developed in [29–35]. In this method, Dissipative Particle Dynamics (DPD) is used to describe the motion of the blood flow and of the platelets, while partial differential equations (PDE) are used for the concentration of blood factors in plasma.

This approach is more appropriate to study clot growth in arteries where the flow velocity is relatively high, and platelet aggregation becomes a dominant factor. We have shown in previous works [27,29] that initial platelet aggregate protects blood factors from the flow, allowing the initiation of fibrin production. On the other hand, fibrin clot reinforces platelet aggregate against the action of the flow.

Since platelets are considered as individual objects, their number and, consequently, the vessel diameter becomes a limiting factor for numerical simulations. In all presented simulations the diameter of the vessel was 50 μm, while the mean flow speed in the undisturbed flow was 12.5 mm/s. The diameter of platelets was set to 2 μm. The density and the viscosity of the simulated medium
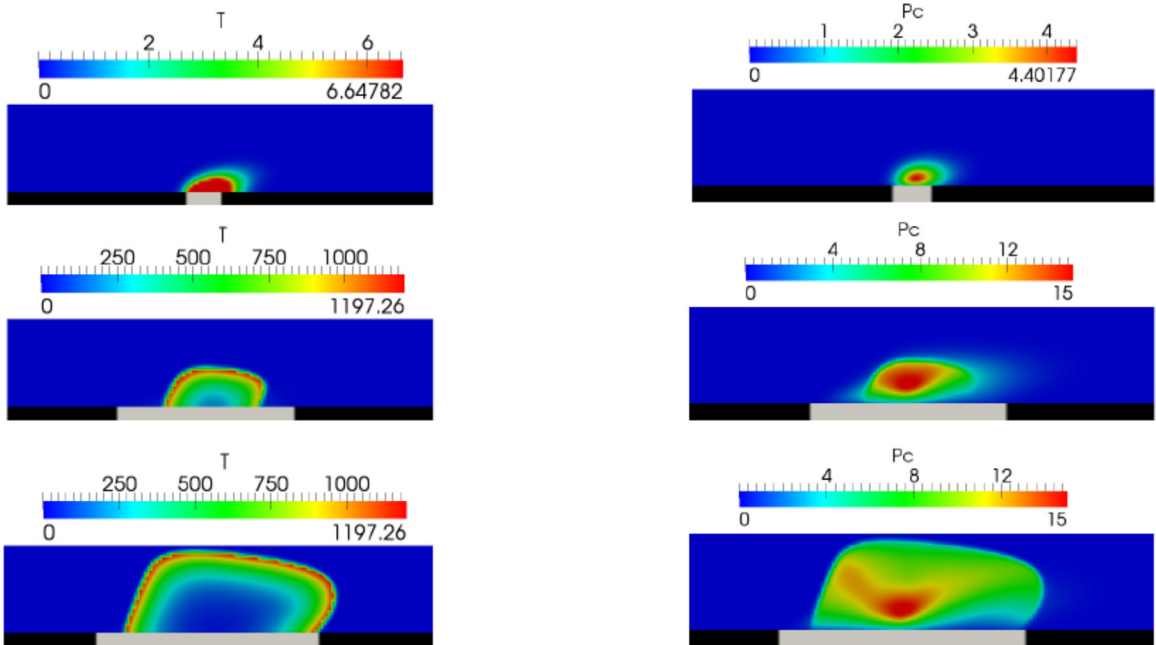

Fig. 5. Snapshot of thrombin distribution (left column) and platelet aggregation (right column) for different sizes of lesions (grey interval at the vessel wall).

Table 1
Values of all the parameters used in the continuous model.

Simulation	Value	Unit	Description
h	0.02	mm	Space step
dt	0.005	s	Time step

Diffusion coefficients	Value	Unit	Description
D	5×10^{-5}	mm^2/s	Blood factors diffusion coefficient [9]
D_p	2.5×10^{-5}	mm^2/s	Platelets diffusion coefficient [9]

Kinetic rates	Value	Unit	Reaction
k_1	5×10^{-7}	nM^{-1} s^{-1}	P activation by ϕ_c [9]
k_2	7.5×10^{-6}	nM^{-1} s^{-1}	P activation by B_a [10]
k_3	1.84×10^{-9}	nM^{-3} s^{-1}	P activation by T (fitted)
k_4	4.817×10^{-6}	nM^{-1} s^{-1}	T inactivation by A [11]
k_5	2.223×10^{-9}	nM^{-1} s^{-1}	B_a inactivation by A [11]
k_6	59	s^{-1}	F_g activation by T [12]
K_6	3160	nM	Substrate fibrin concentration [12]
k_7	0.1	s^{-1}	$F \rightarrow F_p$ fibrin polymerization
k_8	0.17	nM^{-1}	Factor V inactivation by C_a [13]
k_9	0.3	nM^{-1} s^{-1}	Platelets activation by thrombin [14]
k_{10}	0.37	nM^{-1} s^{-1}	Platelets activation by platelets [14]
k_3^*	1.57×10^{-9}	nM^{-3} s^{-1}	P activation by T in the simplified model (fitted)
k_T	1×10^5	nM^{-1}	T binding to TM

Kinetic constants	Value	Unit	Description
α_1	0.0015	nM^{-1} s^{-1}	$\alpha_1 = k_f^- k_f [VII]$
β_1	0.225	nM^{-1}	$\beta_1 = k_f^+ / k_f^-$
α_2	9.4	nM^{-1} s^{-1}	$\alpha_2 = k_c^- k_c$
β_2	100	nM^{-1}	$\alpha_2 = k_c$
ϕ_{max}	12	nM	Maximal density of platelets

Initial concentrations	Value	Unit	Description
P_0	1400	nM	Prothrombin concentration [10]
A_0	3400	nM	Antithrombin concentration [10]
B^0	200	nM	Sum of factors IX and X concentrations [10]
$[VII]$	10	nM	Factor VII concentration [10]
C^0	60	nM	PC concentration [10]
Fg_0	7000	nM	Fibrinogen concentration [10]
ϕ_f^0	10	nM	Platelets density [10]
ϕ_c^0	0.001	nM	Activated platelets bound to the inflamed tissues [10]

Flow properties	Value	Physical	Description
ρ	1.06×10^{-6}	kg mm^{-3}	Blood density
ν	3	mm^{-2} s^{-1}	Blood viscosity
α	100×10^{-6}	mm	Fiber radius
a	5.6×10^{-4}	s mm^{-1}	Thrombin removal rate by flow in the simplified model (fitted)

correspond to the density of viscosity of blood plasma [27,29,34]. A more complete list of values of model parameters is given in Table 1.

A typical clot structure is shown in Fig. 6a. There are three types of platelet connections, weak (light red lines between their centers), medium (dark red lines), and strong (black lines). Medium connections appear if platelets are weakly connected during the time period t_c. Hence we model platelet activation and emergence of medium connections as a time delay. Platelets covered by fibrin are shown with dark green color, platelets not covered by fibrin with light green. Weak and medium platelet connection can be disrupted by flow. In this case, individual platelets or their aggregates can be detached and roll over the clot or leave the clot completely. Platelets covered by fibrin polymer (strong connection) cannot be detached.

Fig. 6b shows results of simulations for three different cases of coagulation initiated by inflammation. The images show the final stages of clot growth for different sizes of inflamed areas. Inflamed parts of the vessel wall are shown in red. In the first case, the inflamed site is short and situated at the bottom wall. In the second and third cases, the inflamed site is longer, and is situated at the bottom wall and both walls respectively. In the second case, the clot was occupying the whole length of the inflamed site; however, a part of it has been detached by the flow.

In all three cases shown in Fig. 6b, the coagulation process and the platelet adhesion at the inflamed site result from the presence of IL-17 in blood at the critical concentration. Fig. 7 shows an example of evolution of a complete vessel occlusion under condition of reduced flow speed. In the simulation, both vessel walls are inflamed, resulting in platelet aggregation on both sides of the vessel, as blood clotting occurs at both vessel walls (the formation of the fibrin net).
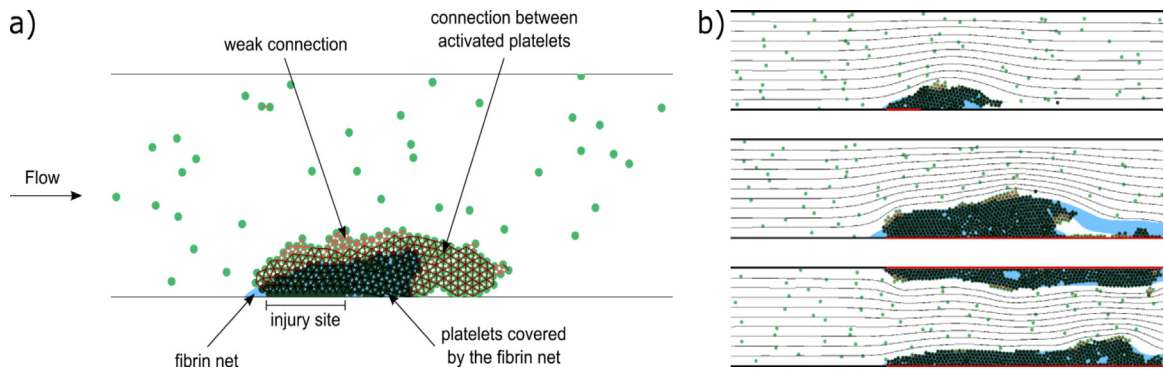
Fig. 6. (a) A scheme of clot structure (snapshot from a simulation). The connections between platelets are shown as red intervals between their centers. Light red lines correspond to weak GPIb connections, dark red to medium connections between activated platelets, and black to strong connections between platelets covered by a fibrin net. Dark green platelets are covered by a fibrin net, which is shown in blue [34]. (b) Final stages of clot growth for different sizes of inflamed areas of vessel wall (shown in red). From top to bottom: short inflamed area at the bottom wall, long area at the bottom wall, long area at both walls. The black lines denote flow streamlines.
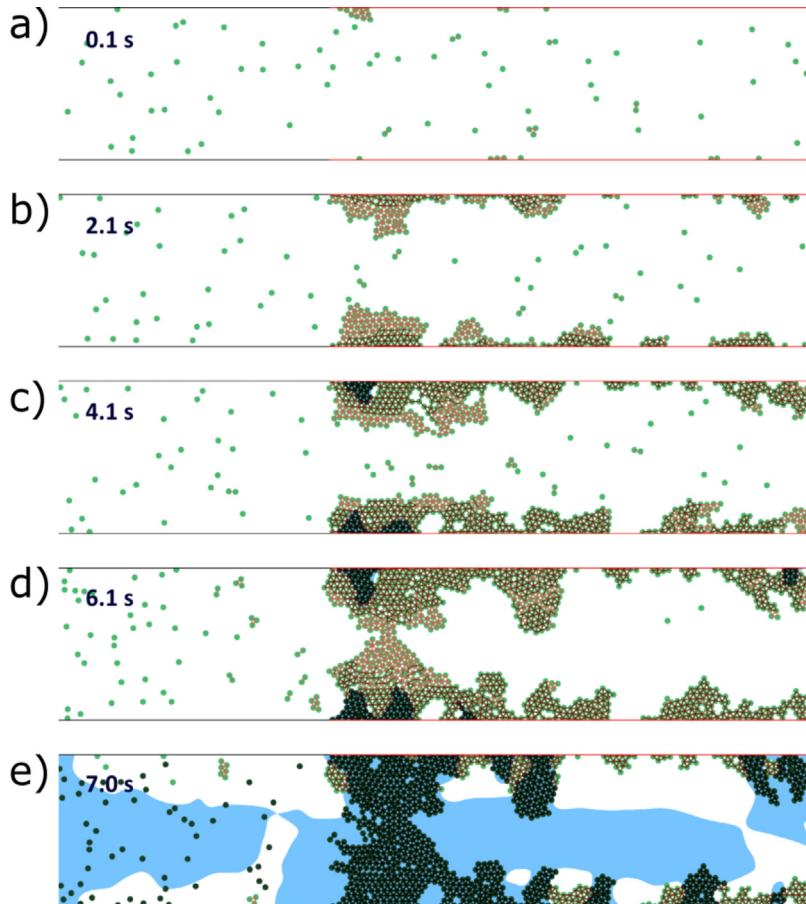

Fig. 7. Vessel occlusion in the case of inflamed walls on both sides and of reduced flow speed. The inactivated platelets begin to aggregate at the inflamed parts of the vessel walls. After a short time delay, they activate and reinforce their connections (a and b). Flow velocity decreases inside the platelet aggregate, stimulating the accumulation of thrombin near the wall and production of fibrin polymer (c). The latter makes platelet connection unbreakable by the flow and leads to further growth of the platelet clot. The flow speed decreases, allowing thrombin production inside the vessel. Finally, the fibrin polymer fills the vessel, resulting in its complete occlusion (d and e). Green dots are platelets; the blue color shows the region with high concentration of fibrin polymer.

4. Conditions of occlusion

In this section, we reduce the complete model presented in the appendix to a simplified model that admits an analytical solution and explicit conditions of vessel occlusion:

- the reaction–diffusion system of equations describing the distribution of blood factors is reduced to a single equation for thrombin concentration;
- the blood flow velocity is approximated by the Poiseuille (parabolic) profile;
- the distributions of factors IX and X initiating thrombin production near the vessel wall due to tissue factor are taken in the stationary form to which they converge after a long time;
- the platelets are considered to be exclusively activated by soluble thrombin.

As a result of these approximations, we obtain the following equation for thrombin concentration:

$$\frac{\partial T}{\partial t} = D \frac{\partial^2 T}{\partial y^2} + \varPhi(T, y), \tag{4.1}$$

where

$$\varPhi(T, y) = (k_1^* T \phi_0 + k_2 B_a(y) + k_3^* T^3)(P_0 - T) - \gamma(y)T,$$

D is the diffusion coefficient, P_0 is the prothrombin concentration initially present in the blood flow, the first term on the right-hand side of the equation describes prothrombin activation by platelets, the second one denotes its activation by factors IX, X ($B_a(y)$), the third term represents the generation of thrombin the amplification phase. The function $\gamma(y) = k_4 A_0 T + a\ v(y)T$ shows the influence of antithrombin and of flow velocity $v(y) = 4v_{\mathrm{m}}y(H-y)/H^2$ in the downregulation of thrombin production. Here H is the width of the vessel, v_{m} is the maximal flow velocity at its axis. The function $B_a(y)$ describes the distribution of factors IXa and Xa. It is a solution to the equation:

$$B_a'' - k_7 A_0 B_a = 0, \qquad B_a'(0) = \frac{\alpha T_{\mathrm{f}}(B^0 - B_a)}{1 + \beta(B^0 - B_a)} \tag{4.2}$$

given in the form $B_a(y) = \lambda e^{-y/\sigma}$, where $\sigma = 1/\sqrt{k_7 A_0}$, and λ can be found from the boundary condition.

Eq. (4.1) is considered in the interval $0 < y < H$, which corresponds to the cross section of the vessel, with the no-flux boundary conditions:

$$y = 0, \quad H : \frac{\partial T}{\partial y} = 0. \tag{4.3}$$

The simplified model gives a good approximation of the speed of clot growth in a quiescent plasma and of the conditions of vessel occlusion in flow [33,36]. In this work, we use this approach to study the influence of inflammation on clot growth. To further simplify the study, the activation of prothrombin by platelets will not be considered in what follows. Fig. 8 (left) shows a comparison of the thrombin distributions in the complete model (appendix) and in the simplified model (4.1) and (4.2). The distribution of thrombin propagates in space due to a self-accelerating cascade of coagulation reactions. In the case of the complete model (solid curves), the concentration of thrombin is measured at the center of the clot in the direction perpendicular to the vessel wall. Thrombin distribution has a specific form, with a maximum at the reaction front and with a gradual decay behind it, due to its elimination by antithrombin. The 1D model shows the same dynamics with the same speed of propagation, but the thrombin profile is monotone in space since the single equation model cannot describe the concentration decay. Except for this difference, it gives a good quantitative approximation of the complete model. Let us note that in the case under consideration, the value of parameter k_3^* in the simplified model is fitted, since it effectively takes into account the influence of activated protein C on clot growth.

In order to analyze clot growth described by Eq. (4.1), we begin with a particular case where the function $\varPhi(T, y)$ is replaced by the function

$$\varPhi_0(T) = k_3^* T^3 (P_0 - T) - k_4 A_0 T.$$

This means that we neglect the boundary effects of clot initiation and the blood flow (quiescent plasma). If $P_0^3 < (27 k_4 A_0)/(4 k_3^*)$, then this function has three zeros, $T = 0$ and T_1, T_2, where $T_0 < T_1 < T_2$. The equilibria $T = 0$ and
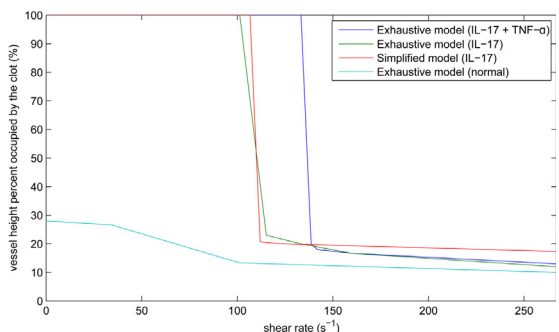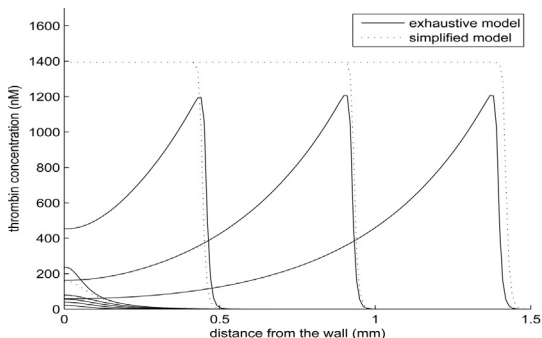

Fig. 8. Thrombin distribution at successive moments of time in the complete model at the middle line of the clot perpendicular to the vessel wall (solid line) and in the one-dimensional approximate model (dashed line) (left). Final clot size as a function of the maximal flow velocity in the complete model (right).

$T = T_2$ are stable as solutions to the corresponding ODE, while $T = T_1$ is unstable. Thus, we obtain a classical reaction–diffusion equation in the bistable case. If it is considered on the whole axis, it has traveling wave solutions, which are solutions of the form $T(x, t) = W(x - ct)$, where W is a solution to the equation

$$DW'' + cW' + \Phi_0(W) = 0, \quad W(-\infty) = T_2, \quad W(\infty) = 0,$$

and c is the speed of propagation. In the case of a positive speed c, such solution describes clot growth. It is known that the wave speed is positive if and only if

$$\int_{T_0}^{T_2} \Phi_0(T) \, dT > 0. \tag{4.4}$$

If we consider the boundary effects and a parabolic velocity distribution, then the function $\Phi(T, y)$ depends on the space variable y, and the problem is considered on the interval $0 < y < H$, which corresponds to the cross section of the vessel in the direction perpendicular to the walls located at $y = 0$ and $y = H$. In this case, the traveling wave solution cannot be defined in the strict mathematical sense, and we consider its approximation. We assume that the wave front (thrombin distribution) is sufficiently sharp. This assumption is biologically realistic due to a strong self-acceleration to the thrombin production. Then we consider a quasi-stationary approximation of the wave for each y fixed. This approximation allows us to formulate an explicit condition of clot growth. Instead of condition (4.4), we now have the inequality

$$I(y) \equiv \int_{T_0}^{T_2} \Phi(T, y) \, dT > 0, \tag{4.5}$$

where T_0 and T_2 depend, in general, on y. This condition can be satisfied for some values of y and not satisfied for some other values. The clot starts growing if $I(0) > 0$, and stops growing if $I(y_0) \leq 0$ for some $y_0 > 0$.

Condition (4.5) shows the influence of the boundary and of the flow on clot initiation and propagation. The function $B_a(y)$ describes the distribution of factors IX and X and their contribution to thrombin production. It increases the function $\Phi(T, y)$ near the wall and promotes the initiation of clot growth. However, it decays exponentially and its influence becomes negligible sufficiently far from the vessel wall. On the contrary, the flow velocity $v(y)$ is low near the wall and attains its maximal value at the axis of the vessel. It decreases the function $\Phi(T, y)$, removing thrombin from the reaction zone. Therefore, the blood flow acts to stop clot growth. If $I(H/2) \leq 0$, then the flow velocity is high enough to stop clot growth. Otherwise, clot overpasses the axis of the flow with the maximal flow velocity, and it continues to grow until it reaches the opposite vessel wall. This case corresponds to complete vessel occlusion.

The explicit form of the condition $I(0) > 0$ allows us to determine the critical concentration of tissue factor at the wall for which clot growth begins:

$$T_f^* = \frac{\lambda^*(e^{-h/\sigma} - 1)}{h\alpha_1(B^0 - \lambda^* e^{-h/\sigma})} \left(1 + \beta_1(B^0 - \lambda^* e^{-h/\sigma})\right). \tag{4.6}$$

Here

$$\lambda^* = \frac{1}{k_2(P_0 - T_2/2)} \left(k_1\phi_0(P_0 - T_2/2) + k_3^* T_2^3(P_0/4 - T_2/5) - k_4 A_0 T_2/2\right).$$

Since inflammation essentially increases the expression of tissue factor at the vessel wall, it can initiate clot growth.

Next, we express from (4.5) the flow speed as a function of the space point y that stops clot growth:

$$v_1(y) = \frac{1}{a} \left(2k_2 B_a(y)\frac{P_0}{T_2} - k_2 B_a(y) + k_3\frac{T_2^2 P_0}{2} - 2k_3\frac{T_3^3}{5} - k_4 A_0\right). \tag{4.7}$$

If $v_1(y)$ exceeds $v(y) = v_m y(H - y)$ for some values of y, then the blood flow stops clot growth, otherwise complete occlusion occurs. Fig. 8 (right) shows a comparison of the numerical simulations of the complete model with the analytical results. The size of the clot (percentage of the vessel cross section) is shown as a function of the maximal flow velocity. For the complete model, the maximal velocity changes in the process of clot growth. So the maximal velocity is taken at the initial moment of time when the velocity profile is the same as in the approximate model. The green line shows the results of numerical simulations of the complete model where only IL-17 is taken into account, and the blue line for the combination of IL-17 and TNF-α. The red line shows the results obtained using the analytical formula. It gives a good approximation of the complete model.

We observe a sharp transition from the complete occlusion to a finite clot size with the increase of flow velocity. Such transition was also observed in in vitro experiments [31]. The combined effect of IL-17 and TNF-α acts more strongly to promote complete occlusion.

5. Discussion

This study quantifies the effects of IL-17 and TNF-α on thrombus development. In order to investigate the effects of these inflammatory cytokines on blood coagulability, we have firstly simulated thrombin generation tests for patients with RA, as described in another study [30], using a previously developed model of blood coagulation [37]. The obtained results were used to determine the levels of tissue factor, thrombomodulin, and CD39 expression in RA patients compared to healthy individuals. These levels were incorporated into two different models of blood clotting to describe the spatiotemporal dynamics of clot growth during inflammatory diseases. As expected, numerical simulations using both models show that blood hypercoagulability, caused by inflammatory cytokines, can lead to thrombosis and vessel occlusion. Especially when the actions of IL-17 and TNF-α are combined.

To examine the association between inflammatory diseases and deep venous thrombosis, we have studied the dynamics of clot growth under venous flow conditions. In such conditions, platelets recruitment and detachment do not play a major role in the pathogenesis of thrombosis. Hence, we have used a continuous modeling approach to describe the blood flow as well as the distributions of

clotting factors and the density of platelets. One of the key features of this model is that it can be reduced to a single equation model that has approximately the same solution. In addition, the reduced model sustains analytical investigation and provides the exact patho-physiological conditions of clot growth initiation and vessel occlusion. Among the conclusions derived from both numerical simulations and analytical results, we observe that the individual action of TNF-α is not sufficient to ensure the occlusion of the vessel. On the other hand, the individual action of IL-17 may trigger venous occlusion when the size of the inflamed tissue is sufficiently large. Overall, the model predicts a higher chance of vascular occlusion when the actions of IL-17 and TNF-α are combined, which is in a good agreement with available clinical data [1,2].

Since platelets aggregation play a key role in the pathogenesis of arterial thrombosis, we have used a different model to describe the effects of IL-17 and TNF-α on clot growth in arteries. The DPD–PDE model, which uses a particle method to describe the interaction between flow and platelets, is a realistic representation of the dynamics of thrombus development under high shear flow. In such hemodynamical conditions, thrombin is washed out by flow, but platelets still manage to aggregate and form unstable clots known as white thrombi. The development of these aggregates is reinforced by IL-17 and TNF-α due to the overexpression of CD39, which ultimately results in the obstruction of the blood flow by the platelet plug. Only then, the fibrin polymer mesh can expand and solidify the thrombus. A comparison of the two models indicates that the upregulation of CD39 expression due to IL-17 and TNF-α is more crucial in the formation of arterial thrombi than venous ones.

Although the models presented in this study provide key insights into the development of thrombosis during RA and other inflammatory diseases, they are still based on several assumptions. Some of these assumptions concern the coagulation cascade, a concept that was first introduced as 'Y'-shaped waterfall where the intrinsic and the extrinsic pathways come together into a common pathway, leading to the production of thrombin and the subsequent generation of the fibrin mesh [38]. We reduced it in order to capture the essential dynamics of blood clotting when initiated by the extrinsic pathway. In this regard, the amplification phase was assumed to depend solely on thrombin, while in reality, it involves other factors such as V, VIII, XI, and XII. Furthermore, in both models, we consider the vessel walls to be rigid and the blood flow to be driven by a constant nonpulsatile pressure difference. These simplifications were necessary since the main objective of this study is to quantify the effects of inflammatory cytokines and not to study the interactions between thrombus formation, the blood flow, and the vessel walls. We also consider a constant blood flow rate instead of pulsatile one. Blood flow pulsations have high frequency compared to the characteristic time of clot growth. So we expect that an averaged flow velocity can give a good approximation. However, this is not yet verified in the DPD–PDE model. Flow pulsations can influence platelet aggregation and activation. We will introduce blood pulsations in the forthcoming works.

Moreover, we restrict the present study to 2D modeling of thrombus formation. The development of 3D models of thrombus formation requires the implementation of different numerical methods than the ones used for the discretization of the current models. It also requires the numerical validation through comparison with the 2D model results. These questions will be addressed in a subsequent work. Finally, in the present study, we identify inflammatory diseases effects on blood clotting by the exclusive actions of IL-17 and TNF-α, while in reality, these diseases alter the levels of other clotting factors such as factor VII and I, among others [39]. The quantification of such mechanisms does not fall into the scope of the present study.

While each of the two models presented in this work has its strengths and disadvantages, both of them are necessary to quantify the procoagulant roles of IL-17 and TNF-α in different contexts. The development of these models was inspired by existing experimental studies. However, in order to fully understand and quantify the association between inflammation and thrombosis, more studies combining clinical experiments and numerical simulations are necessary. In particular, the development of a systems biology framework is essential for building more validated mathematical models that can be used to accurately predict the risk of thrombosis in individual patients.

Arterial thrombosis basically occurs due to the rupture of a atherosclerotic plaque, while venous thromboembolism is mostly related to stasis, hypercoagulation, and endothelial damage [40]. This difference is probably related to different hemodynamic conditions in veins, arteries, including blood flow velocity and blood pressure [41]. In both cases, RA and PsA can trigger endothelial inflammation, resulting in plaque formation in arteries and thromboembolism in veins. Further development of the disease depends on the size of the lesions. Mathematical modeling of atherosclerosis shows that inflamed region grows in time as a reaction-diffusion wave [42–45]. It is followed by vessel remodeling and possible plaque rupture due to its interaction with the blood flow.

Plaque formation in the case of arterial inflammation is much slower than thrombus formation. However, a high flow velocity can prevent thrombus formation. A slower blood flow in veins allows thrombus initiation, and the latter probably prevents plaque formation.

The approximate analytical model does not contain explicitly the lesion size. It is present implicitly in the parameters of the model characterizing the rate of thrombin production. Since this simplified model gives a good approximation of the complete model, then we can expect that it can be used to predict thrombosis development in individual patients. This approach can also be used to model thrombosis treatment [46].

Classical CV risk factors related to obesity, hypertension, smoking, etc., have been identified for a long time. Such conclusion has been obtained from the study of long-term cohorts, the most famous cohort being that used for the Framingham study. However, these studies have their own limitations including their descriptive nature and the limitations to provide explanations for the observed changes. One way to provide such answers is to use

cohorts from conditions where the CV risk is increased. This will reduce the follow-up duration. At the same time this will allow the collection of biosamples for better biological studies.

Acknowledgements

References

[1] A. Hot, F. Lavocat, V. Lenief, P. Miossec, Simvastatin inhibits the pro-inflammatory and pro-thrombotic effects of IL-17 and TNF-α on endo-thelial cells, Ann. Rheum. Dis. 72 (5) (2013) 754–760.

[2] A. Hot, V. Lenief, V.P. Miossec, Combination of IL-17 and TNF-α induces a pro-inflammatory, pro-coagulant and pro-thrombotic phenotype in human endothelial cells, Ann. Rheum. Dis. 71 (5) (2012) 768–776.

[3] J.A. Avina-Zubieta, H.K. Choi, M. Sadatsafavi, M. Etminan, J.M. Esdaile, D. Lacaille, Risk of cardiovascular mortality in patients with rheumatoid arthritis: a meta-analysis of observational studies, Arthritis Care Res. 59 (12) (2008) 1690–1697.

[4] S.I. van Leuven, R. Franssen, J.J. Kastelein, M. Levi, E.S. Stroes, P.P. Tak, Systemic inflammation as a risk factor for atherothrombosis, Rheumatology 47 (1) (2008) 3–7.

[5] S. Hannawi, B. Haluska, T.H. Marwick, R. Thomas, Atherosclerotic disease is increased in recent-onset rheumatoid arthritis: a critical role for inflammation, Arthritis Res. Ther. 9 (4) (2007) R116.

[6] I.A. Ku, J.B. Imboden, P.Y. Hsue, P. Ganz, Rheumatoid arthritis: model of systemic inflammation driving atherosclerosis, Circ. J. 73 (2009) 977–985.

[7] F. Wolfe, B. Freundlich, W.L. Straus, Increase in cardiovascular and cerebrovascular disease prevalence in rheumatoid arthritis, J. Rheumatol. 30 (1) (2003) 36–40.

[8] W. Marder, S. Khalatbari, J.D. Myles, R. Hench, S. Yalavarthi, S. Lustig, S.M.J. Kaplan, Interleukin 17 as a novel predictor of vascular function in rheumatoid arthritis, Ann. Rheum. Dis. 70 (9) (2011) 1550–1555.

[9] E. Smith, K.M. Prasad, M. Butcher, A. Dobrian, J.K. Kolls, K. Ley, E. Galkina, Blockade of interleukin-17A results in reduced atherosclerosis in apolipo-protein E-deficient mice, Circulation 121 (15) (2010) 1746–1755.

[10] S. Chen, K. Shimada, W. Zhang, G. Huang, T.R. Crother, M.M. Arditi, IL-17A is proatherogenic in high-fat diet-induced and *Chlamydia pneumoniae* infection-accelerated atherosclerosis in mice, J. Immunol. 185 (9) (2010) 5619–5627.

[11] S. Hashmi, Q.T. Zeng, Role of interleukin-17 and interleukin-17-in-duced cytokines interleukin-6 and interleukin-8 in unstable coronary artery disease, Coron. Artery Dis. 17 (8) (2006) 699–706.

[12] A. Bouchnita, T. Galochkina, V. Volpert, Influence of antithrombin on the regimes of blood coagulation: insights from the mathematical model, Acta Biotheor. 64 (2016) 327–342.

[13] M. Anand, K. Rajagopal, K.R. Rajagopal, A model for the formation and lysis of blood clots, Pathophysiol. Haemos. Thromb. 34 (2-3) (2005) 109–120.

[14] K.G. Mann, C. Van't Veer, K. Cawthern, S. Butenas, The role of the tissue factor pathway in initiation of coagulation, Blood Coagul. Fibrinolysis 9 (1998) S3–7.

[15] A.L. Fogelson, N. Tania, Coagulation under flow: the influence of flow-mediated transport on the initiation and inhibition of coagulation, Pathophysiol. Haemost. Thromb. 34 (2-3) (2005) 91–108.

[16] S.E. Harrison, J. Bernsdorf, D.R. Hose, P.V. Lawford, A lattice Boltzmann framework for simulation of thrombogenesis, Prog. Comput. Fluid Dyn. 8 (1-4) (2008) 121–128.

[17] W. Stortelder, P.W. Hemker, H.C. Hemker, Mathematical modelling in blood coagulation; simulation and parameter estimation, Rep. Model. Anal. Simul. 20 (1997) 1–11.

[18] G.P. Galdi, R. Rannacher, A.M. Robertson, S. Turek, Hemodynamical Flows. Modeling, Analysis and Simulation, Birkhauser, Basel, 2008.

[19] A.I. Lobanov, T.K. Starozhilova, The effect of convective flows on blood coagulation processes, Pathophysiol. Haemost. Thromb. 34 (2–3) (2006) 121–134.

[20] N. Bessonov, A. Sequeira, S. Simakov, Y. Vassilevskii, V. Volpert, Methods of blood flow modelling, Math. Model. Nat. Phenom. 11 (1) (2016) 1–25.

[21] A. Tokarev, I. Sirakov, G. Panasenko, V. Volpert, E. Shnol, A. Butylin, F. Ataullakhanov, Continuous mathematical model of platelet thrombus formation in blood flow, Russ. J. Numer. Anal. Math. Model. 27 (2) (2012) 191–212.

[22] T. Bodnar, A. Sequeira, M. Prosi, On the shear-thinning and viscoelastic effects of blood flow under various flow rates, Appl. Math. Comput. 217 (11) (2011) 5055–5067.

[23] K. Leiderman, A.L. Fogelson, Grow with the flow: a spatial-temporal model of platelet deposition and blood coagulation under flow, Math. Med. Biol. 28 (1) (2011) 47–84.

[24] A.L. Fogelson, R.D. Guy, Immersed-boundary-type models of intravascular platelet aggregation, Comput. Methods Appl. Mech. Eng. 197 (25) (2008) 2087–2104.

[25] Z. Xu, S. Christley, J. Lioi, O. Kim, C. Harvey, W. Sun, M. Alber, Multiscale model of fibrin accumulation on the blood clot surface and platelet dynamics, Methods Cell Biol. 110 (2012) 367–388.

[26] N. Bessonov, E. Babushkina, S.F. Golovashchenko, A. Tosenberger, F. Ataullakhanov, M. Panteleev, V. Volpert, Numerical modelling of cell distribution in blood flow, Math. Model. Nat. Phenom. 9 (6) (2014) 69–84.

[27] A. Tosenberger, F. Ataullakhanov, N. Bessonov, M. Panteleev, A. Tokarev, V. Volpert, Modelling of thrombus growth in flow with a DPD–PDE method, J. Theor. Biol. 337 (2013) 30–41.

[28] N. Filipovic, M. Kojic, A. Tsuda, Modelling thrombosis using dissipative particle dynamics method, Philos. Trans. R. Soc. Lond. A: Math. Phys. Eng. Sci. 366 (1879) (2008) 3265–3279.

[29] A. Tosenberger, F. Ataullakhanov, N. Bessonov, M. Panteleev, A. Tokarev, V. Volpert, Modelling of platelet-fibrin clot formation in flow with a DPD–PDE method, J. Math. Biol. 72 (3) (2016) 649–681.

[30] A. Undas, M. Gissel, B. Kwasny-Krochin, P. Gluszko, K.G. Mann, K.E. Brummel-Ziedins, Thrombin generation in rheumatoid arthritis: dependence on plasma factor composition, Thromb. Haemost. 104 (2) (2010) 224.

[31] F. Shen, C.J. Kastrup, Y. Liu, R.F. Ismagilov, Threshold response of initiation of blood coagulation by tissue factor in patterned microfluidic capillaries is controlled by shear rate, Arterioscler. Thromb. Vasc. Biol. 28 (11) (2008) 2035–2041.

[32] A.V. Belyaev, M.A. Panteleev, F.I. Ataullakhanov, Threshold of microvascular occlusion: injury size defines the thrombosis scenario, Biophys. J. 109 (2) (2015) 450–456.

[33] A. Bouchnita, T. Galochkina, P. Kurbatova, P. Nony, V. Volpert, Conditions of microvessel occlusion for blood coagulation in flow, Int. J. Numer. Methods Biomed. Eng. (2016).

[34] A. Tosenberger, N. Bessonov, V. Volpert, Influence of fibrinogen deficiency on clot formation in flow by hybrid model, Math. Model. Nat. Phenom. 10 (1) (2015) 36–47.

[35] A. Tosenberger, F. Ataullakhanov, N. Bessonov, M. Panteleev, A. Tokarev, V. Volpert, Modelling of thrombus growth in flow with a DPD–PDE method, J. Theor. Biol. 337 (2013) 30–41.

[36] T. Galochkina, H. Ouzzane, A. Bouchnita, V. Volpert, Traveling wave solutions in the mathematical model of blood coagulation, Appl. Anal. (2016) 1–15.

[37] A. Bouchnita, A. Tosenberger, V. Volpert, On the regimes of blood coagulation, Appl. Math. Lett. 51 (2016) 74–79.

[38] E.W. Davie, O.D.O.D. Ratnoff, Waterfall sequence for intrinsic blood clotting, Science 145 (3638) (1964) 1310–1312.

[39] A. McEntegart, H.A. Capell, D. Creran, A. Rumley, M. Woodward, G.D.O. Lowe, Cardiovascular risk factors, including thrombotic variables, in a population with rheumatoid arthritis, Rheumatology 40 (6) (2001) 640–644.

[40] E. Previtali, P. Bucciarelli, S.M. Passamonti, I. Martinelli, Risk factors for venous and arterial thrombosis, Blood Transfus. 9 (2) (2011) 120–138.

[41] H. Zhang, A. Sun, Y. Shen, J. Jia, S. Wang, K. Wang, J. Ge, Artery interposed to vein did not develop atherosclerosis and underwent atrophic remodeling in cholesterol-fed rabbits, Atherosclerosis 177 (1) (2004) 37–41.

[42] N. El Khatib, S. Genieys, B. Kazmierczak, V. Volpert, Reaction–diffusion model of atherosclerosis development, J. Math. Biol. 65 (2) (2012) 349–374.

[43] N. El Khatib, S. Genieys, A.M. Zine, V. Volpert, Non-Newtonian effects in a fluid–structure interaction model for atherosclerosis, J. Tech. Phys. 1 (50) (2009) 55–64.

[44] N. El Khatib, S. Genieys, B. Kazmierczak, V. Volpert, Mathematical modelling of atherosclerosis as an inflammatory disease, Philos. Trans. R. Soc. Lond. A: Math. Phys. Eng. Sci. 367 (1908) (2009) 4877–4886.

[45] N. El Khatib, S. Genieys, V. Volpert, Atherosclerosis initiation modeled as an inflammatory process, Math. Model. Nat. Phenom. 2 (2) (2007) 126–141.

[46] A. Bouchnita, K. Bouzaachane, T. Galochkina, P. Kurbatova, P. Nony, V. Volpert, An individualized blood coagulation model to predict INR therapeutic range during warfarin treatment, Math. Model. Nat. Phenom. 11 (6) (2016) 28–44.

Appendix A. Mathematical model

A.1. PDE model

A.1.1. Reaction-diffusion equations for blood factors

We extend a previously developed model of clot growth dynamics [1,2] to include the aggregation of platelets. The model consists of reaction-advection-diffusion equations describing the spatiotemporal distributions of blood coagulation factors during thrombus development:

Prothrombin

$$\frac{\partial P}{\partial t} + \nabla \cdot (vP) = D\Delta P - \left(k_1\phi_c + k_2 B_a + \frac{k_3 T^3}{1 + k_8 C_a}\right)P, \quad \text{(A.1)}$$

Thrombin

$$\frac{\partial T}{\partial t} + \nabla \cdot (vT) = D\Delta T$$
$$+ \left(k_1\phi_c + k_2 B_a + \frac{k_3 T^3}{1 + k_{10} C_a}\right)P - k_4 AT, \quad \text{(A.2)}$$

Factors IXa, Xa

$$\frac{\partial B_a}{\partial t} + \nabla \cdot (vB_a) = D\Delta B_a - k_5 AB_a, \quad \text{(A.3)}$$

APC

$$\frac{\partial C_a}{\partial t} + \nabla \cdot (vC_a) = D\Delta C_a - k_c C_a, \quad \text{(A.4)}$$

Antithrombin

$$\frac{\partial A}{\partial t} + \nabla \cdot (vA) = D\Delta A - k_4 AT - k_5 AB, \quad \text{(A.5)}$$

Fibrinogen

$$\frac{\partial F_g}{\partial t} + \nabla \cdot (vF_g) = D\Delta F_g - \frac{k_6 TF_g}{K_6 + F_g}, \quad \text{(A.6)}$$

Fibrin

$$\frac{\partial F}{\partial t} + \nabla \cdot (vF) = D\Delta F + \frac{k_6 TF_g}{K_6 + F_g} - k_7 F, \quad \text{(A.7)}$$

Fibrin polymer

$$\frac{\partial F_p}{\partial t} = k_7 F. \quad \text{(A.8)}$$

Platelets in flow

$$\frac{\partial \phi_f}{\partial t}$$
$$+ \nabla \cdot (k(\phi_c)v\phi_f)$$
$$= k(\phi_c)D_p\Delta(\phi_f) - k_9 T\phi_f - k_{10}\phi_f\phi_c, \quad \text{(A.9)}$$

Platelets in clot

$$\frac{\partial \phi_c}{\partial t} + \nabla \cdot (k(\phi_c)v\phi_c) = k(\phi_c)D_p\Delta(\phi_c) + k_9 T\phi_f$$
$$+ k_{10}\phi_f\phi_c, \quad \text{(A.10)}$$

Here v is flow velocity, D is the diffusion coefficient, which is taken the same for all proteins, and $k(\phi_c)D_p$ is the effective diffusion coefficient for platelets, where $k(\phi_c) = \tanh(\pi(1 - \frac{\phi_c + \phi_f}{\phi_{max}}))$ a decreasing function. Fibrin polymer forms a solid clot, it does not diffuse and it is not transported by flow.

A.1.2. Boundary conditions

In order to describe the generation of thrombin in the initiation phase at the damaged endothelial wall, we consider the complex T_f^* formed by the tissue factor and factor VII. Factors IX and X interact with this complex due to a surface reaction. They come from the bulk solution being inactive, form a complex T_f^*B with T_f^* and return to the solution in the active form. The reaction rate for the surface concentration of this complex can be written as follows:

$$\frac{\partial [T_f^*B]}{\partial n} = k_f^+ B(T_f^* - [T_f^*B]) - k_f^- [T_f^*B],$$

where the first term in the right-hand side of this equation describes the flux of B to the surface, the second term describes the flux from the surface. Assuming that this reaction is fast, we can use the detailed equilibrium:

$$k_f^+ B(T_f^* - [T_f^*B]) = k_f^- [T_f^*B].$$

Then

$$[T_f^*B] = \frac{k_f B T_f^*}{1 + k_f B}, \quad \text{(A.11)}$$

where $k_f = k_f^+/k_f^-$.

The boundary conditions for the variables B and B_a at the damaged surface are as follows:

$$\frac{\partial B}{\partial n} = -k_f^+ B(T_f^* - [T_f^*B]), \quad \frac{\partial B_a}{\partial n} = k_f^- [T_f^*B], \quad \text{(A.12)}$$

We prescribe the zero flux condition at the intact surface.

In order to simplify the boundary conditions, let us introduce the variable $z = B + B_a$. From Eq. (A.12) and the boundary conditions for B and B_a we get:

$$\frac{\partial z}{\partial t} + \nabla \cdot (vz) = D\Delta z - k_b z, \quad \frac{\partial z}{\partial n} = 0. \quad \text{(A.13)}$$

Assuming that initially $B + B_a = B^0$, where B^0 is the initial concentration of factors IX and X, we conclude that the solution of problem (A.13) is identically constant, $B + B_a = B^0$. Hence we can exclude the variable B from the equations and from the boundary condition:

$$\frac{\partial B_a}{\partial n}\Big|_{\Gamma_d} = \frac{\alpha_1(B^0 - B_a)}{1 + \beta_1(B^0 - B_a)}, \quad \text{(A.14)}$$

where $\alpha_1 = k_f^- k_f T_f^*$ and $\beta_1 = k_f$.

Protein C is activated by the complex of thrombin-thrombomodulin. The fluxes of protein C at the surface in its active and inactive forms are given as follows:

$$\frac{\partial C}{\partial n} = -k_c^+ C([TT_m] - [CTT_m]), \quad \frac{\partial C_a}{\partial n} = k_c^- [CTT_m].$$

Here $[T_m]$ is the concentration of thrombomodulin present at the undamaged surface. Protein C arrives next to thrombin and thrombomodulin and forms the complex CTTm. Here k_8^+ is the reaction rate constant of protein C activation by the complex of thrombin thrombomodulin, k_c^- is the rate of the inverse reaction. Again using the detailed equilibrium, we obtain the condition of APC production on undamaged walls:

$$\frac{\partial C_a}{\partial n}\Big|_{\Gamma_u} = \frac{\alpha_2(C^0 - C)[TT_m]}{1 + \beta_2(C^0 - C_a)}, \tag{A.15}$$

$$[TT_m] = \frac{k_T[TT_m]}{1 + k_T[TT_m]}, \tag{A.16}$$

where $\alpha_2 = k_c^- k_c$ and $\beta_2 = k_c$, $[TT_m]$ is the complex thrombin thrombomodulin that activates protein C present in blood plasma. We consider the no-flux boundary conditions for these concentrations at the other parts of the boundary, and also for other concentrations. In the case of nonzero flow velocity, the concentrations of prothrombin, fibrinogen and antithrombin at the entrance of the domain ($x = 0$) are kept constant.

A.1.3. Blood flow model

To incorporate the action of blood flow on clot growth, we use the Navier–Stokes equations to describe the dynamics of blood flow in the vessel.

$$\rho\left(\frac{\partial \vec{v}}{\partial t} + \vec{v}\nabla\vec{v}\right) = -\nabla p + \mu\Delta\vec{v} - \frac{\mu}{K_f(\vec{x})}\vec{v}, \tag{A.17}$$

$$\nabla\vec{v} = 0,$$

where $\vec{v} = (v_x, v_y)$ is the velocity vector, p is the pressure, ρ the density of blood, μ the kinematic viscosity. H the height of the vessel. In this work, we consider a laminar incompressible flow. K_f is the hydraulic permeability of fibrin polymer [3]:

$$\frac{1}{K_f(\vec{x})} = \frac{16}{\alpha^2} F_p^{1.5}(1 + 56F_p(\vec{x})^3)\left(\frac{1 + \phi_c(\vec{x})}{1 - \phi_c(\vec{x})}\right). \tag{A.18}$$

Here F_p- and ϕ_c- are the normalized concentration of fibrin polymer and density of platelets in the clot respectively, α is the fiber radius of the fibrin polymer mesh.

The effects of red blood cells (RBCs) on thrombus formation are taken implicitly through the choice of viscosity similarly to the other continuous models of thrombus growth. RBCs and fibrin are the main components of venous thrombus. For this reason, we refer to those thrombi as red clots due to the red color of RBCs. RBCs exhibit two features that have an impact on the rheology of the blood. First, RBCs aggregate under low shear flow and form stacks due to their discoid shape. This increases the overall viscosity of the blood flow [4]. The other mechanical property of RBCs is their deformability under high shear flows. This property has an

adverse effect on the viscosity of the blood flow with respect to RBCs aggregation. The influence of RBCs can be properly captured using cell-based models of blood flow. In such models, blood is described as a heterogeneous fluid consisting of both plasma and blood cells. These models become complex and computationally expensive. To our knowledge, a model that considers the effects of RBCs on thrombus growth in flow does not exist yet due to the complexity of such modeling.

We prescribe the no-slip boundary conditions for the velocity at the upper and lower walls, and periodic boundary conditions in the axial direction. The blood flow is driven by the pressure difference. Therefore, we use periodic boundary conditions for velocity coupled with a constant pressure difference condition:

$$p_{in} = p_{out} + \Delta p, \tag{A.19}$$

where p_{in} is the pressure at the inlet, p_{out} is the outlet pressure and Δp is the pressure difference which is considered as an imposed constant. Contrary to the condition of fixed inlet velocity, this imposed pressure difference condition allows the clot to completely occlude the vessel and obstruct the flow. The numerical implementation of the model was presented in [2].

A.1.4. Model reduction

Let us consider the simplified model:

$$\frac{\partial v_1}{\partial t} = D\Delta v_1 + \widehat{k}_1 T - h_1 v_1, \tag{A.20}$$

$$\frac{\partial v_2}{\partial t} = D\Delta v_2 + \widehat{k}_2 T - h_2 v_2, \tag{A.21}$$

$$\frac{\partial v_3}{\partial t} = D\Delta v_3 + \widehat{k}_3 T - h_3 v_3, \tag{A.22}$$

$$\frac{\partial v_4}{\partial t} = D\Delta v_4 + \widehat{k}_4 v_3 - h_4 v_4, \tag{A.23}$$

$$\frac{\partial v_5}{\partial t} = D\Delta v_5 + \widehat{k}_5 v_4 + k_1^c v_2 v_4 - h_5 v_5, \tag{A.24}$$

$$\frac{\partial T}{\partial t} = D\Delta T + \left(\widehat{k}_6 v_5 + k_2^c v_1 v_5\right)P - \sigma T \tag{A.25}$$

obtained as an approximation of the more complete model of blood coagulation in quiescent platelet-free plasma [5,6]. Here T denotes thrombin concentration, T_0 is its maximal concentration equal to the initial concentration of prothrombin. The variables v_i, $i = 1, \ldots, 5$ correspond to the concentrations of active forms of the factors V, VIII, XI, IX and X, respectively. The coefficients $\widehat{k}_i$ denote activation reaction rates, and h_i inhibition rates. Factors VIIIa and IXa form the intrinsic kinase complexes [VIIIa,IXa], while factors Va and Xa form the prothrombinase complex [Va,Xa]. They further accelerate thrombin production. They enter Eqs. (A.23) and (A.24) in the form $k_1^c v_2 v_4$ and $k_2^c v_5 v_1$ obtained under the assumption of detailed equilibrium. This system of equations should be completed by the

equations of fibrin production from fibrinogen (activated by thrombin) and fibrin polymer production from fibrin. These equations do not influence the equations of thrombin production, so that the system (A.20)–(A.24) can be considered independently.

Under the assumption of detailed equilibrium (large reaction constants) we express the variables $v_1, \ldots, v_5$ from Eqs. (A.20)–(A.23):

$$v_1 = \frac{\widehat{k}_1}{h_1}T, \quad v_2 = \frac{\widehat{k}_2}{h_2}T, \quad v_3 = \frac{\widehat{k}_3}{h_3}T, \quad v_4 = \frac{\widehat{k}_3\widehat{k}_4}{h_3 h_4}T,$$
$$v_5 = \frac{\widehat{k}_3\widehat{k}_4}{h_3 h_4}T\left(\frac{\widehat{k}_5}{h_5} + \frac{k_1^c \widehat{k}_2}{h_2 h_5}\ T\right) \tag{A.26}$$

and substitute them into the last equation. We get the single reaction–diffusion equation

$$\frac{\partial T}{\partial t} = D\Delta T + bT^3 P - \sigma T, \tag{A.27}$$

where

$$b = \frac{\widehat{k}_1 \widehat{k}_2 \widehat{k}_3 \widehat{k}_4 k_1^c k_2^c}{h_1 h_2 h_3 h_4 h_5}$$

and some small terms are neglected. Taking into account the initiation of thrombin production, its inhibition by activated protein C and platelets, we obtain Eq. (A.2) where $\sigma = k_4 A$ and convective terms are omitted for brevity. In the case of small values of σ, Eqs. (A.1) and (A.2) can be approximated by Eq. (4.1). The concentration B can be found in the quasi-stationary approximation as a solution of the stationary equation (A.3), where the convection term is neglected since the flow velocity is low near the vessel wall (see (4.2)). It was shown in [2,7,8] that a model reduction gives a good approximation of the complete model.

A.1.5. Model parameters

A.2. PDE-DPD model

A.2.1. DPD submodel

Dissipative particle dynamics is a mesoscale method in the sense that each DPD particle describes some small volume of a simulated medium rather than an individual molecule [16,18,19]. There are conservative, dissipative, and random forces acting between every two particles:

$$F_{ij}^C = F_{ij}^C(r_{ij})\widehat{r}_{ij}, \qquad F_{ij}^D = -\gamma\omega^D(r_{ij})(v_{ij}\cdot\widehat{r}_{ij})\widehat{r}_{ij},$$
$$F_{ij}^R = \sigma\omega^R(r_{ij})\frac{\xi_{ij}}{\sqrt{dt}}\widehat{r}_{ij},$$

where $\vec{r}_i$ is the vector of position of the particle i,

$$\vec{r}_{ij} = \vec{r}_i - \vec{r}_j, \qquad r_{ij} = |\vec{r}_{ij}|, \qquad \widehat{r}_{ij} = \vec{r}_{ij}/r_{ij},$$

and $v_{ij} = v_i - v_j$ is the difference between velocities of two particles; γ and σ are coefficients that determine the strength of the dissipative and the random forces, respectively, while ω^D and ω^R are weight functions; ξ_{ij} is a normally distributed random variable with zero mean, unit variance, and $\xi_{ij} = \xi_{ji}$. The conservative force is given by the equality

$$F_{ij}^C(r_{ij}) = \begin{cases} a_{ij}(1 - r_{ij}/r_c) & \text{for } r_{ij} \leq r_c, \\ 0 & \text{for } r_{ij} > r_c, \end{cases} \tag{A.28}$$

where a_{ij} is the conservative force coefficient between particles i and j, and r_c is the cutoff radius. If the following two relations are satisfied, system will preserve its energy and maintain the equilibrium temperature:

$$\omega^D(r_{ij}) = \left[\omega^R(r_{ij})\right]^2, \qquad \sigma^2 = 2\gamma k_B T,$$

where k_B is the Boltzmann constant and T is the temperature. The weight functions are determined by:

$$\omega^R(r_{ij}) = \begin{cases} (1 - r_{ij}/r_c)^k & \text{for } r_{ij} \leq r_c, \\ 0 & \text{for } r_{ij} > r_c, \end{cases} \tag{A.29}$$

where $k = 1$ for the original DPD method, but it can be also scaled in order to change the dynamic viscosity of the simulated fluid. The motion of particles is determined by Newton's second law.

It is important to note that all forces between particles are pairwise. Therefore, if we take a closed volume, then all forces between the particles inside it are cancelled. Only the forces from the particles outside act on the volume. These properties characterize hydrodynamics and allow the derivation of macroscopic equations of motion. Under the appropriate choice of parameters, DPD gives results similar to the Navier–Stokes equations, but is much less computationally expensive. Hence, its applications become justified for simulating complex heterogeneous media [15,16].

A.2.2. Platelet aggregation submodel

In order to describe platelets and their aggregation in flow, we consider that some of the particles in the DPD description of the medium are platelets, while other particles simulate lumps of blood plasma. Platelets still remain DPD particles in the sense that DPD forces remain acting on platelets; however, we apply additional rules of interaction between platelets themselves.

First we consider that platelets cannot cross each other, unlike plasma particles, which can pass one through another because of the finite potential force acting between them. In order to prevent platelets from passing through each other, we will introduce an additional linear potential force between them:

$$\mathbf{F}_{ij}^P = \begin{cases} k^P\left(1 - \frac{r_{ij}}{d_P}\right)\widehat{\mathbf{r}}_{ij}, & \text{if } r_{ij} < d_P, \\ \mathbf{0}, & \text{if } r_{ij} \geq d_P, \end{cases} \tag{A.30}$$

where d_P is the platelet diameter, k^P is the force strength coefficient.

Next, we describe platelet aggregation – when two platelets come in physical contact, i.e. the distance between their centers is less then the platelet's diameter ($r_{ij} < d_P$), they establish a weak adhesive connection. Platelet aggregation can be strengthened through the process of platelet activation, during which platelets go through physical changes, developing a pseudopod stellar shape. Moreover, activated platelets initiate the activation of surrounding aggregated platelets. The platelet activation therefore increases stability of the platelet aggregate on the injury site. However, the last step of the clot stabilisation is the result of the coagulation pathways. Fibrin monomers, which are synthesized at the injury site, polymerize, creating a so-called fibrin net, which together with aggregated platelets forms the blood clot, making the aggregate more stable. The stable blood clot then gives time for the underlying tissue to heal.

In order to describe different types of adhesion between platelets, we introduce an adhesion force that acts between connected platelets:

$$\mathbf{F}_{ij}^A = \begin{cases} f^A(t_{ij})\left(1 - \dfrac{r_{ij}}{d_P}\right)\hat{\mathbf{r}}_{ij}, & \text{if } d_P \leq r_{ij} \leq d_D, \\ \mathbf{0}, & \text{if } r_{ij} < d_P \text{ or } r_{ij} > d_D, \end{cases} \quad (A.31)$$

where t_{ij} is the age of the connection between the platelets, while d_D (such that $d_D > d_P$) is the critical distance after which the connection between two platelets is considered to be severed. We define the function $f^A(t_{ij})$ as follows:

$$f^A(t_{ij}) = \begin{cases} k_1^A, & \text{if } F_p(i) \text{ or} F_p(j) < c_{F_p}, \quad \text{and} \quad t_{ij} < t_c, \\ k_2^A, & \text{if } F_p(i) \text{ or} F_p(j) < c_{F_p}, \quad \text{and} \quad t_{ij} \geq t_c, \\ k_3^A, & \text{if } F_p(i) \quad \text{and} \quad F_p(j) \geq c_{F_p}, \end{cases}$$

$$(A.32)$$

where $f_1^A < f_2^A < f_3^A$ are the three strengths of inter-platelet connections, representing respectively a weak bond due to GPIb receptors, a medium bond due to platelet activation, and a strong bond due to reinforcement by fibrin polymer net; t_c is the time needed for platelet activation measured from the moment when the connection is established. As the platelet activation process is not the focus of this study, the activation period serves as a basic approximation of the platelet activation process due to the contact and proximity of other activated platelets (e.g., activation due to the secretion of ADP). $F_p(i)$ and $F_p(j)$ are levels of fibrin polymer F_p at the positions of particles i and j, respectively. The levels of F_p are given by the coagulation sub-model. c_{F_p} is the critical level of fibrin polymer. A platelet is considered to be a part of the clot core if it is in the clot and the fibrin concentration is larger than c_{F_p} at the position of that platelet. Therefore, the clot core is a part of the clot covered by a concentration of F_p larger than c_{F_p}. As the platelets that are coated in fibrin are adhesion-resistant [17], the same condition is applied to the model in a way that the platelets that belong to the clot core cannot establish new connections with the platelets in the flow.

Dissipative Particle Dynamics (DPD) is not a deterministic method due to the random forces between particles. Hence, it is possible to obtain different outcomes when running two numerical simulations with the same sets of parameters. However, the qualitative results of the model remain the same and significant changes of the simulation outcome only occur when parameters are changed. We have presented a detailed sensitivity analysis for the different parameters used in the model in previous works [21,22].

The DPD–PDE model is based on a sophisticated coupling of the DPD method and the resolution of PDEs. This coupling consists in running the two components in parallel and then proceeds to the exchange of data between them. PDEs are solved numerically on a fine using the finite difference method. An accurate quadratic bilinear interpolation is used to compute the concentration of fibrin on the coordinates of each particle. The same interpolation is used to calculate the flow velocity in the PDE mesh.

A.2.3. PDE submodel

Equations for the concentrations of blood factors are similar to the equations presented in Section A.1.1. It is assumed here that the concentration of antithrombin is in excess, and its variation is neglected. The influence of IL-17 and TNF-α on the coagulation cascade is taken into account through the boundary conditions (Section A.1.2). Parameter values used in the DPD and PDE submodels are provided in Table 2.

A.3. A comparative study of arterial thrombus simulation using the continuous and the DPD–PDE models

The mechanisms involved in the development of arterial thrombosis differ from those driving the growth of venous thrombosis. In arterial thrombosis, the high shear flow washes away thrombin and prevents the generation of the fibrin mesh. In this context, platelets are still able to attach to the subendothelium and form a plug. To test the ability of the continuous model in reproducing the dynamics of platelet plug formation, we consider that the porosity of the plug depends solely on the density of platelets in the plug [3]:

$$\frac{1}{K_p(\bar{x})} = \frac{150\,\phi_c}{\Psi^2(2\alpha_p)(1 - \phi_c)^3}, \quad (A.33)$$

where Ψ is the sphericity of a platelet and α_p is its radius. In order to reproduce the experimental conditions [20], we impose a constant parabolic flow velocity at the inlet with a maximum value $v_m = 1250\,\mu\text{m/s}$. As a computational domain, we consider a microvessel with a diameter of $50\,\mu\text{m}$ similar to the one in the DPD–PDE simulations. Using these changes, it is possible to track the evolution of the thrombus under high shear flow using the continuous model presented in Appendix A.1. We show the result for the vessel height occupied by the plug of platelets as well as some screenshots of the simulation in Fig. 9. The shown quantitative results are close to the results of the DPD–PDE

Table 2
Values of all fixed parameters in the basic simulation with the DPD–PDE model.

Domain	Value	Physical	Description
L	250	250 μm	Length of the simulated blood vessel
D	50	50 μm	Diameter of the simulated blood vessel
G_x	7200	72 m/s^2	External force in x direction used to induce flow
v_x	187.5	18.75 mm/s	Average flow velocity
w_x		1500 s^{-1}	Wall shear rate

DPD	Value	Physical	Description
a_{ij}	600,000		Conservative force coefficient
γ	3550		Dissipative force coefficient
σ	20,000		Random force coefficient
r_c	5		Force cut-off radius
k_BT	1		The Boltzmann constant times temperature
n	0.36		Particle number density
m	0.463		Particle mass
dt_{DPD}	0.001		DPD time step

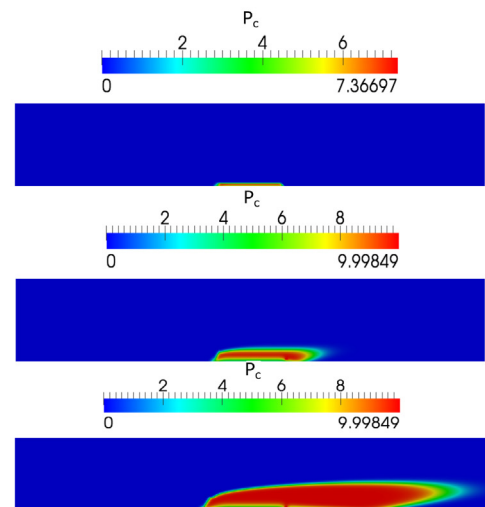| Other	Value	Physical	Description
f_1^A	3×10^6	0.3 nN	Weak inter-platelet bond coefficient
f_2^A	8×10^6	0.8 nN	Activated inter-platelet bond coefficient
f_3^A	1×10^8	10 nN	Fibrin net reinforced bond coefficient
t_c	10	0.1 s	Platelet activation period
τ	10	0.1 s	DPD–PDE data exchange period
p	0.017	3.672×10^{12} L^{-1}	Platelet frequency
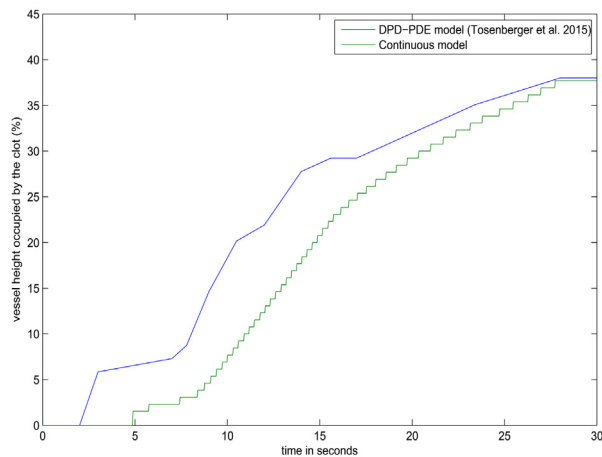
Fig. 9. Numerical simulations of arterial thrombus formation using the continuous model. (a) The vessel height occupied by the platelet plug over time. (b) Screenshots of the simulation corresponding to the $t = 5$ s (top), $t = 10$ s (middle), $t = 20$ s (bottom).

model, although the latter provides a more realistic representation of the formation of unstable white thrombi, since it takes into account the detachment of fragments from the clot.

References of the Appendix

[1] A. Bouchnita, A. Tosenberger, V. Volpert, On the regimes of blood coagulation, Appl. Math. Lett. 51 (2016) 74–79.

[2] A. Bouchnita, T. Galochkina, P. Kurbatova, P. Nony, V. Volpert, Conditions of microvessel occlusion for blood coagulation in flow, Int. J. Numer. Methods Biomed. Eng. (2016).

[3] A.R. Wufsus, N.E. Macera, K.B. Neeves, The hydraulic permeability of blood clots as a function of fibrin and platelet density, Biophys. J. 104 (8) (2013) 1812–1823.

[4] O.K. Baskurt, H.J. Meiselman, Blood rheology and hemodynamics, Semin. Thromb. Hemost. 29 (5) (2003) 435–450.

[5] V.I. Zarnitsina, A.V. Pokhilko, F.I. Ataullakhanov, A mathematical model for the spatio-temporal dynamics of intrinsic pathway of blood coagulation. II. Results, Thromb. Res. 84 (5) (1996) 333–344.

[6] Y.V. Krasotkina, E.I. Sinauridze, F.I. Ataullakhanov, Spatiotemporal dynamics of fibrin formation and spreading of active thrombin entering non-recalcified plasma by diffusion, Biochim. Biophys. Acta (BBA): Gen. Subj. 1474 (3) (2000) 337–345.

[7] T. Galochkina, A. Bouchnita, P. Kurbatova, V. Volpert, Reaction-diffusion waves of blood coagulation, Math. Biosci. 288 (2017) 130–139.

[8] A. Bouchnita, T. Galochkina, V. Volpert, Influence of antithrombin on the regimes of blood coagulation: insights from the mathematical model, Acta Biotheor. 64 (4) (2016) 327–342.

[9] K. Leiderman, A.L. Fogelson, Grow with the flow: a spatial-temporal model of platelet deposition and blood coagulation under flow, Math. Med. Biol. 28 (1) (2011) 47–84.

[10] M.F. Hockin, K.C. Jones, S.J. Everse, K.G. Mann, A model for the stoichiometric regulation of blood coagulation, J. Biol. Chem. 277 (21) (2002) 18322–18333.

[11] E.M. Wiebe, A.R. Stafford, J.C. Fredenburgh, J.I. Weitz, Mechanism of catalysis of inhibition of factor IXa by antithrombin in the presence of heparin or pentasaccharide, J. Biol. Chem. 278 (37) (2003) 35767–35774.

[12] M. Tsiang, L.R. Paborsky, W.X. Li, A.K. Jain, C.T. Mao, K.E. Dunn, D.W. Lee, S.Y. Matsumura, M.D. Matteucci, S.E. Coutré, L.L. Leung, C.S. Gibbs, Protein engineering thrombin for optimal specificity and potency of anticoagulant activity in vivo, Biochemistry 35 (51) (1996) 16449–16457.

[13] S. Solymoss, M.M. Tucker, P.B. Tracy, Kinetics of inactivation of membrane-bound factor Va by activated protein C. Protein S modulates factor Xa protection, J. Biol. Chem. 263 (29) (1988) 14884–14890.

[14] A.L. Kuharsky, A.L. Fogelson, Surface-mediated control of blood coagulation: the role of binding site densities and platelet deposition, Biophys. J. 80 (3) (2001) 1050–1074.

[15] D.A. Fedosov, I.V. Pivkin, G.E. Karniadakis, Velocity limit in DPD simulations of wall-bounded flows, J. Comput. Phys. 227 (4) (2008) 2540–2559.

[16] R.D. Groot, P.B. Warren, Dissipative particle dynamics: bridging the gap between atomistic and mesoscopic simulation, J. Chem. Phys. 107.11 (1997) 4423–4435.

[17] M.M. Kamocka, J. Mu, X. Liu, N. Chen, A. Zollman, B. Sturonas-Brown, K. Dunn, Z. Xu, D.Z. Chen, M.S. Alber, E.D. Rosen, Two-photon intravital imaging of thrombus development, J. Biomed. Opt. 15 (1) (2010) 016020-016020.

[18] M. Karttunen, I. Vattulainen, A. Lukkarinen, A Novel Methods in Soft Matter Simulations, Springer, Berlin, 2004.

[19] S.Y. Trofimov, Thermodynamic Consistency in Dissipative Particle Dynamics, Eindhoven University Press, 2003.

[20] S. Falati, P. Gross, G. Merrill-Skoloff, B.C. Furie, B. Furie, Real-time in vivo imaging of platelets, tissue factor and fibrin during arterial thrombus formation in the mouse, Nat. Med. 8 (10) (2002) 1175–1180.

[21] A. Tosenberger, F. Ataullakhanov, N. Bessonov, M. Panteleev, A. Tokarev, V. Volpert, Modelling of thrombus growth in flow with a DPD–PDE method, J. Theor. Biol. 337 (2013) 30–41.

[22] A. Tosenberger, F. Ataullakhanov, N. Bessonov, M. Panteleev, A. Tokarev, V. Volpert, Modelling of platelet-fibrin clot formation in flow with a DPD–PDE method, J. Math. Biol. 72 (3) (2016) 649–681.